Open access Journal International Journal of Emerging Trends in Science and Technology

Comparative Study of VOC Sensors Based on Ruthenated MWCNT/SnO_2 Nanocomposites

Authors

Vladimir Aroutiounian[1], Zaven Adamyan[2], Artak Sayunts[3], Emma Khachaturyan[4] Arsen Adamyan[5], Klara Hernadi[6], Zoltan Nemeth[7], Peter Berki[8]

[1,2,3,4,5]Yerevan State University, Center of Semiconductor Devices and Nanotechnologies, 1, A. Manoukian, Yerevan 00, Armenia

[6,7,8]University of Szeged, Department of Applied and Environmental Chemistry, Rerrich B. tér 1, 6720 Szeged, Hungary

Corresponding Author

Vladimir Aroutiounian

Yerevan State University, Center of Semiconductor Devices and Nanotechnologies, 1, A. Manoukian, Yerevan 00, Armenia

Email**:** *Aroutiounv1@gmail.com*

Abstract

Thick-film VOCs sensors based on ruthenated multi-walled carbon nanotubes coated with tin-dioxide nanoparticles nanocomposite structures (MWCNTs/SnO_2) are prepared using three methods: hydrothermal synthesis, sol–gel technique and their combined process. Properties prepared nanocomposite powders are characterized by TEM and SEM techniques. It is shown that the optimal conditions for applications as acetone, toluene, ethanol and methanol vapors sensors in view of high response and selectivity relative to each other depend on choice of material synthesis method, mass ratio of the nanocomposite components and selected operating temperature. MWCNTs/SnO_2 sensor structures having the mass ratio of the components 1:4 and 1:24 exhibit selective sensitivity to acetone and toluene vapors at 150^oC operating temperature, respectively. The samples with 1:200 mass ratio of the nanocomposite components show the selective and response to acetone vapor exposure in the range of 200-250^oC operating temperatures. The high sensitivity to ethanol and methanol vapors at 200^oC operating temperature was revealed for the sensor structures made by all three proposed methods with the 1:8, 1:24, 1:50 and 1:66 ratio of the components.

Keywords: *MWCNTs/SnO_2, VOCs, sensor acetone, toluene, ethanol, methanol*

1. Introduction

Up-to-date advancement of the sensing technology is generated a need of mankind safety and security as well as monitoring of air pollution. So, air pollution influences human health and can cause a number of diseases. The main air pollutants are some inorganic gases (e.g. CO, NO_x, and SO_2) as well as various volatile organic compounds (VOCs). Toxic and pollutant VOCs such as acetone, toluene, and formaldehyde are found in indoors. The main sources of the same VOCs in outdoor are industrial emissions, combustion processes, traffic vehicles and fuel evaporation [1]. In indoor environments such as homes, workplaces, cars and shopping centers, these contaminants originate from building materials such as paints, varnish thinners, coatings and furniture [2]. Since, the probability of over exposure to these contaminants now is very high, gas sensing devices' installation in such places and develop of advanced monitoring systems for their early detection are necessary.

The VOCs detection may also be applied in breathalyzers and medical processes such as disease diagnoses and controlling. Some VOCs

such as acetaldehyde, ethanol, methanol and acetone [3]–[5] are dangerous else because they do not only pollute the environment but also break down to more toxic substances directly deteriorate human's health depending on such a VOCs used amount [6],[7]. So, ethanol used in drink reduces human's consciousness and reaction and becomes a major cause of car accidents. In addition, acetaldehyde is formed in the body as a result of mucosal and microbial oxidation of ethanol [8]. But, it is known that acetaldehyde itself is an irritant of the skin, eyes, mucous membranes, throat, and respiratory tract. This occurs at concentrations up to 1000 ppm. Symptoms of exposure to this compound include nausea, vomiting, headache.

Acetone widely used in industries and labs. It is extensively used to dissolve plastic, purify paraffin, and dehydrate tissues in pharmaceutics. Inhalation of acetone causes headache, fatigue and even narcosis and harmfulness to nerve system.

Acetone is another important VOCs in breath. Highly sensitive acetone gas sensors are essential for identification of diabetes and monitoring health conditions and treatment of diabetic patients [9],[10]. As a case in point, if the maximum acetone concentration in breath more than 1.8 ppm could indicate high ketone level in blood symptom of insulin-dependent diabetes [3],[11].

The rapid and sensitive analysis of acetone gas concentration in human breath is a key technique for noninvasive diagnosis of diabetes. The traditional gas chromatography system as well as calorimetric and optical methods [12],[13] or some others [14] used for this purpose is expensive and requires special knowledge for operation [15], which is not suitable for real-time measurements.

Gas sensors based on nanostructured semiconductor metal-oxides materials such as nanoparticles [16]-[18], nanowires [19]-[21], nanobelts [22], polycrystalline nanotubes [23], nanorods [24], hollow spheres and nanofibers [25],[26], 3D aloe-like [26] and/or their nanocomposites with carbon nanotubes (CNTs) [28]-[32] are considered as the most promising for applications in gas detection systems and devices. CNTs in itself possess by a number of useful behaviors such as a wide range of electrical properties, small size, high structural and chemical stability, high strength and so on. Dew to introduction of CNTs to metal-oxide matrix or deposition of metal-oxide nanoparticles on the nanotubes walls, specific surface area of such gas-sensitive nanocomposites increases still more. Moreover, additional nanochannels in the form of hollow CNTs for gas diffusion appear [33]-[35]. Hence, it can be expected that application of nanocomposite hybrid structures composed of functionalized CNTs and metal oxide in gas sensors technology should improve the gas sensor parameters, particularly, gas sensitivity, response and recovery times as well as reduce the operating temperatures.

As a gas-sensitive materials meant for the use in high performance gas sensor applications both taken separately and as a component of hybrid system, researches have mainly focused their efforts on n-type nanostructured metal-oxides such as SnO_2, In_2O_3, ZnO, WO_3, TiO_2 and their compounds [3]-[7],[9],[11],[15]-[18]. Among them, SnO_2 is the most prospective and widely used gas-sensitive material for the gas sensor to detect a wide variety of pollutant gases dew to its attractive features including high gas sensitivity, relatively low specific resistance and operating temperatures, chemical durability, low cost, nontoxicity, and simple preparation [36].

In previous works [31],[32], we had shown that the functionalization of multi-walled carbon nanotube (MWCNT)/SnO_2 with thick-film structures by Ru leads to considerable increase in response signal to methanol and ethanol vapors as well as to i-butane gas. However, the selectivity problem of studied sensors relative to other gases, particularly to some harmful and toxic VOCs exposure remained not solved. The goal of present work is bring to light on optimal conditions at which the best level of the selectivity these sensors to various VOCs achieves.

In this paper, we report the some VOCs sensing properties of various ruthenated MWCNT/SnO_2 nanocomposite structures as thick films obtained

by hydrothermal synthesis and sol-gel techniques as well as theirs combination. The choice of corresponding treating conditions and regimes for CNTs functionalization as well as thick films surface modification with Ru catalyst were focused on obtaining the sensitivity to such target gases as ethanol, methanol, acetone and toluene.

2. Materials and samples preparation

2.1. Materials preparation

MWCNTs/SnO_2 nanopowders for thick film preparation were made by the following three ways: using sol–gel preparation technique, hydrothermal synthesis and their two-step combination.

To making the nanocomposite structures according to the first way, MWCNTs membranes were used for preparation of nanocrystalline MWCNTs/SnO_2 powder. MWCNTs were prepared by the decomposition of acetylene (CVD method) using Fe, Co/$CaCO_3$ catalyst [37,38]. This growth procedure using $CaCO_3$ catalyst enables a highly efficient selective formation of clean MWCNTs, suitable for effective bonding between CNT and metal-oxide, particularly, SnO_2 precursors.

For a functionalization of nanotube walls with oxygen-containing hydroxyl (OH), carbonyl (C=O), and carboxylic (COOH) functional groups, MWCNTs from the membranes were transferred to slurry in HNO_3/H_2SO_4 acids mixture during 1 h. Such a functionalization of the CNTs is very important and necessary for the following synthesis of SnO_2 nanoparticles on the MWCNTs walls since these oxygen-containing groups act as sites for the nucleation of nanoparticles. After rinsing by distilled water and drying at 80 ^oC, MWCNTs were poured and treated in deionized water in ultrasonic bath for 5 min.

In the next step, the purified MWCNT and the calculated water solution of the $SnCl_4 \cdot 5H_2O$ precursor were mixed for a further 5 h at 140^oC. After that, precipitate was collected for the following synthesis of hybrid material. For that, the precursor solution was added to all of the precipitate. Obtained mixture was exposed to ultrasonic treatment for 5 min. The mixed suspension was left overnight at 80 ^oC, whereupon MWCNTs/SnO_2 composite powder with 0.1% addition of the MWCNTs was rinsed, dried, grinded and annealed in air at 400 ^oC for 1 h. The final mass ratio of MWCNTs/SnO_2 composite was 1:50, respectively. This sol-gel process is presented elsewhere [31], in detail.

The preparation of SnO_2/MWCNT nanocomposite materials with a hydrothermal method was carried out in two steps. The preparation of nanocomposite materials with a hydrothermal method was carried out in two steps. At first, purified MWCNTs was well dispersed in water via sonication. After that, a calculated amount of the $SnCl_2 \cdot 2H_2O$ precursor was dissolved in another beaker in water, whereupon 3 cm^3 HCl was added to the solution. In the next step, the MWCNT suspension and the solution of the precursor were mixed and sonicated for 30 min. In order to prepare the nanocomposites we poured the above-mentioned solutions into autoclaves where hydrothermal synthesis was carried out at 150 ^oC for 1 day. At the end of this procedure, all obtained nanocomposite powders were filtered and then dried at 90 ^oC for 5h. The final mass ratios of the MWCNT/SnO_2 nanocomposite obtained with the hydrothermal method were 1:4, 1:8, 1:66, and 1:200, respectively.

The third type of composite material using both hydrothermal and wet chemical methods was obtained by following route. Firstly, we were prepared 45 ml 0.5M $SnCl_4$ $5H_2O$ deionized water solution. Then, 11 mg hitherto obtained MWCNT/SnO_2 powder synthesized by above-mentioned hydrothermal method was added to the solution with thorough mixing by a magnetic stirrer. Simultaneously, ammonium was added drop by drop to the solution at 42^oC on reaching pH=9. After that, the solution was left in the thermostat at 80^oC for 24 hours. Resulting slurry with deionized water addition was centrifuged at a spinning rate of 7000 rpm with further washing of the precipitates. Spinning and washing processes were carried out as long as chlorides in the

solution disappear entirely. Then, the purified from chlorides sediment was left at 140°C overnight. Obtained powder was annealed in air at 400°C for 3 hours. The final mass ratio of obtained by such a way MWCNTs/SnO_2 composite components was 1:24, respectively.

The chose water as a solvent, instead of e.g. ethanol, in all presented here three material preparation methods was preferably for us in the view of expected improvement in gas sensing characteristics, taking in account the fact that cover the overwhelming parts of CNTs with SnO_2 nanoparticles is ensured at that [39].

2.2. Samples

The thick films were obtained on the base of all MWCNTs/SnO_2 composite powders. The paste for the thick film deposition made by mixing powders with α-terpineol ("Sigma Aldrich") and methanol was printed on chemically treated surface of the alumina substrate over the ready-made Pt interdigitated electrodes. The thin-film Pt heater was formed on the back side of the substrate. Obtained composite structures were cut into 3×3 mm pieces. Drying and annealing of the resulting thick films were carried out in two stages: heating up to 220°C with 2°C min^{-1} rate of temperature rise, hold this temperature for 3 h and then further temperature increase until 400°C with 1°C min^{-1} rate and hold again for 3 h. Then, the thick-film specimens were cooled down in common with the oven.

After annealing and cooling processes, the MWCNTs/SnO_2 thick films were surface-ruthenated by dipping its into the 0.01 M $RuOHCl_3$ aqueous solution for 20 min whereupon dried at 80°C for 30 min and then annealing treatment was carried out again at the same above-mentioned mode. The choice of the ruthenium as a catalyst was defined by its some advantages [31]. Further, ruthenated MWCNT/SnO_2 chips were arranged in TO-5 packages and after leads bonding offered gas sensors were ready to measurements.

2.3. Gas sensing measurements

VOCs vapors sensing properties of the MWCNTs/SnO_2 composite structures were measured by home-made developed computer-controlled static gas sensor test system [40]. The sensors were re-heated at different operating temperatures. When the resistances of all the sensors were stable, saturated target vapor was injected into a measurement chamber by a microsyringe. The target gases including, ethanol, methanol, acetone, toluene vapor were introduced in the measurement chamber on special hot plate designed for the quickly conversion of the liquid substance to its gas phase (≤12 s). After the sensor resistances reached a new constant value, the test chamber was opened to recover the sensors in air. The sensing characteristics were studied at a temperature range of 100-300°C. The gas response S, of the sensors was defined as R_a/R_g where R_a and R_g are the electrical resistances in air and in target VOCs-air mixed gas, respectively. The response and recovery times are determined as the time required for reaching 90% resistance change from the corresponding steady-state value of the signal.

The volume part of the gas in air was calculated by the following equation [41]:

$$C_{ppm} = \frac{\rho \times V_l \times R \times T}{M \times P_v \times V_{ch}} \times 10^6$$

where ρ (g/cm^3) is the density of injected liquid, V_l is the volume of the injected liquid, R is the universal gas constant, T is the absolute temperature, M (g/mol) is the molecular weight, P_v is the pressure after the vaporization of the injected liquid, V_{ch} is the volume of the chamber.

3. Results and discussions

3.1. Material characterization

The morphologies of the prepared SnO_2/MWCNT nanocomposite different powders were studied by the scanning electron microscopy (SEM) using Hitachi S-4700 Type II FE-SEM equipped with a cold field emission gun operating in the range of 5–15 kV. The samples were mounted on a conductive carbon tape and sputtered with a thin Au/Pd layer in Ar atmosphere prior to the measurement.

Fig. 1 shows SEM image of the pristine carbon nanotubes lying in the MWCNTs membrane. The rough estimation of the CNTs sizes shows that the

average diameter of carbon nanotubes not covered with SnO_2 nanoparticles clusters is about 25 nm.

In previous published results [31], we were shown that with increasing the weight ratio of the MWCNT/SnO_2 nanocomposite components from 1:4 to 1:50 the inorganic coverage of carbon nanotubes becomes thicker and thicker. Comparison of these results with ones obtained for the samples with the weight ratios 1:66 and 1:200 were verified this tendency.

The micrograph for specimen with the 1:4 weight the ratio of the components presented in Fig. 2 shows that spherical tin oxide nanoparticles covered the CNTs are well dispersed and separated from each other whereas in the case of the 1:66 one (see Fig.3) SnO_2 nanoparticles are conjugated into the clusters. .

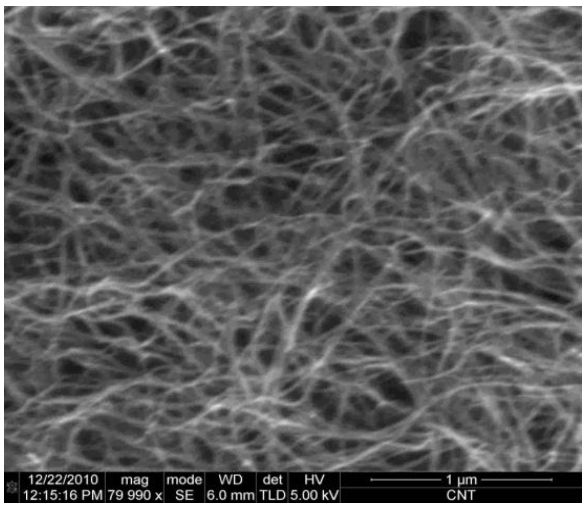

Fig. 1 SEM image of the pristine CNTs.

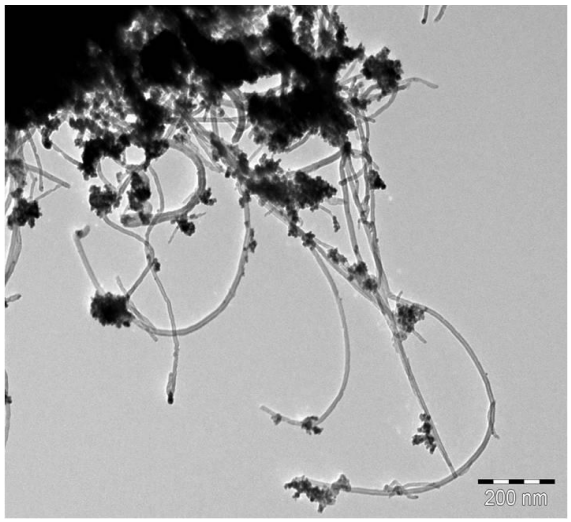

Fig.2. TEM image of MWCNT/SnO_2 nanocomposite with the 1:4 ratio of the components.

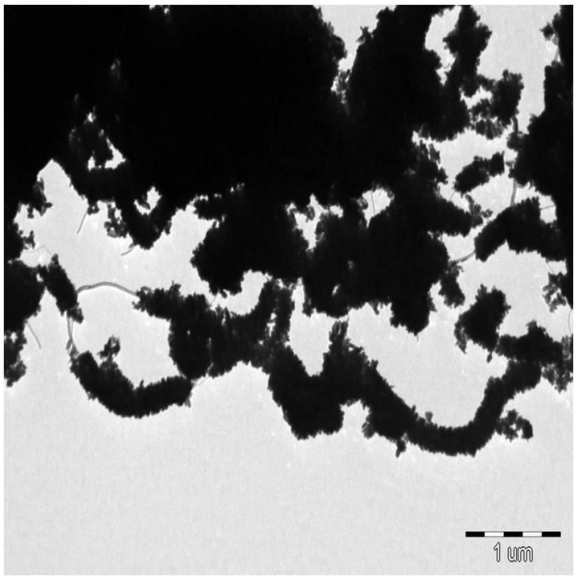

Fig.3. TEM image of MWCNT/SnO_2 nanocomposite with the 1:66 ratio of the components.

The presence of an oxide layer was confirmed by SEM-EDX and the crystalline structure of the inorganic layer was also studied by an X-ray diffraction method using Rigaku Miniflex II diffractometer (angle range: 2θ [^{o}] =10–80 utilizing characteristic X-ray (CuKα) radiation). Results of these studies are presented in [31] in detail. Here, we are only noted that average crystalline size of SnO_2 nanoparticles are less than 12 nm for all using synthesis methods.

3.2. Gas sensing characteristics

At first, we consider the response from presence of methanol and ethanol vapors in the measurement chamber atmosphere. As a result of our studies, we were revealed that the most response from these alcohols inherent to sets of MWCNT/SnO_2 nanocomposite samples made by all mentioned above material synthesis methods with corresponding ratios of the components beginning from 1:8 up to 1:200, at 200^{o}C operating temperature. Results of these measurements and samples codes with corresponding synthesis methods are summarized in Table 1 and bar chart (Fig.4) below.

Table 1. The response of studied MWCNT/SnO_2 samples to 1000 ppm of different gases at 200°C operating temperature.

Sample code	Process parameters	R_{air}/R_{meth}	R_{air}/R_{eth}
KCS1-3	Hydrothermal synthesis, 1:4	22	14
KCS2-2	Hydrothermal synthesis, 1:8	1500	500
EKCS3-2	Hybrid method, 1:24	1000	750
ECS7-2	Sol-gel, 1:50	1000	2000
ZCS-66	Hydrothermal synthesis, 1:66	700	600
ZCS-200	Hydrothermal synthesis, 1:200	384	400

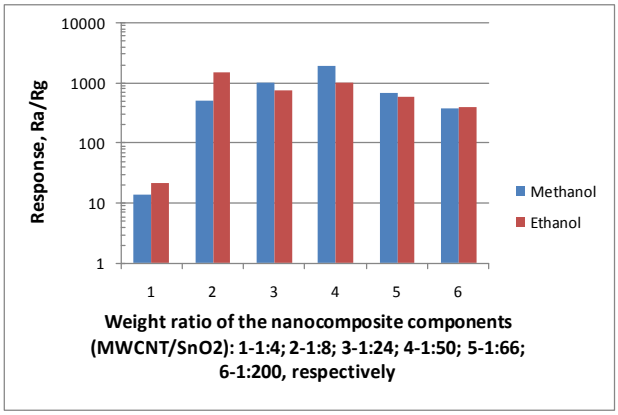

Fig.4. Response to 1000 ppm methanol and ethanol vapors at 200°C operating temperature.

It can be seen from diagram, beginning from 1:8 weight ratio of the nanocomposite components up to one 1:50, sensors response to methanol and ethanol vapors not vary practically. Moreover, we can assert that in this range of weight ratio of the nanocomposite components, the sensors made by using the mentioned above different three technologies react to these alcohols something like. But, further increase in the SnO_2 component of the nanocomposite result in gradual decrease in ethanol and methanol vapors responses. Nevertheless, sensitivity to these alcohols vapor remains as long as high. As distinct from previous study [31], here we consider the more range of weight ratio of the nanocomposite components as well as addition of new hybrid nanocomposite synthesis method. Results of our investigations were shown that the sensitivity of studied sensors to methanol and ethanol vapors not so much depends from material synthesis methods as rather than sensors operating temperature and required definite amount of SnO_2 nanoparticles covered with MWCNTs walls.

It should be noted that 200°C is optimal operating temperature for detection of methanol and ethanol vapors by such nanocomposite sensors. But, we were set ourselves as an object to find conditions and corresponding material technology at which the best selectivity to one or another gases achieves. With this purpose, we were carried out the testing of all samples at different operating temperatures in other to compare responses to various considered here target VOCs. Results of these investigations fulfilled for set of ECS7-2 series samples summarized in Fig. 5. The relatively high 1000 ppm concentration is chosen for selectivity better shows.

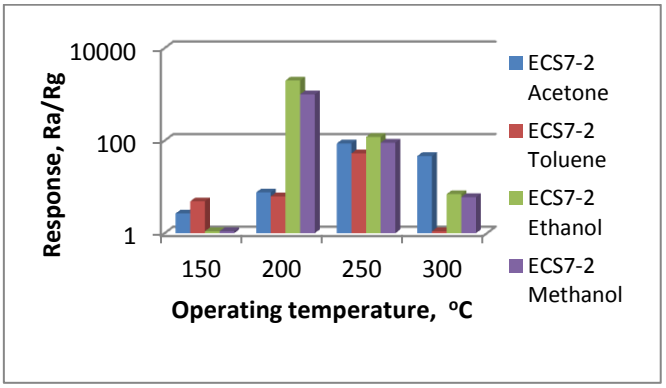

Fig. 5. Comparison of ECS7-2 series sample responses to 1000 ppm different VOC exposure vs operating temperature.

It is obvious that the best selectivity relative to other VOC and high response values are registered at methanol and ethanol vapors exposure at 200°C operating temperature. Unfortunately, separate detection of methanol and ethanol vapors is not come in as yet. There is not selectivity at 250°C operating temperature though at that relatively

high response observed for all target VOCs. While, the same series samples are shown the sufficiently selective detection of acetone vapors at 300°C.

Taking into account the fact that KCS1-3 set of samples with 1:4 ratio of the nanocomposite components also selectively sensitive to the alcohols only at 200°C but with lesser responses, we were hoped obtaining selective sensitivity to acetone or toluene vapors at lower or higher operating temperatures. The responses of KCS1-3 samples to studied VOCs vs operating temperature is presented in Fig.6. It can be seen that the selective sensitivity these samples to acetone vapors at the same concentration of all vapors is observed as early as at 150°C operating temperature. With the increase in the operating temperature, the response to acetone vapor rises up to 360.4 value at 250°C while selectivity remains high. Undoubtedly, functioning at lower operating temperature (150°C) with ensuring the best selectivity is preferably in all cases.

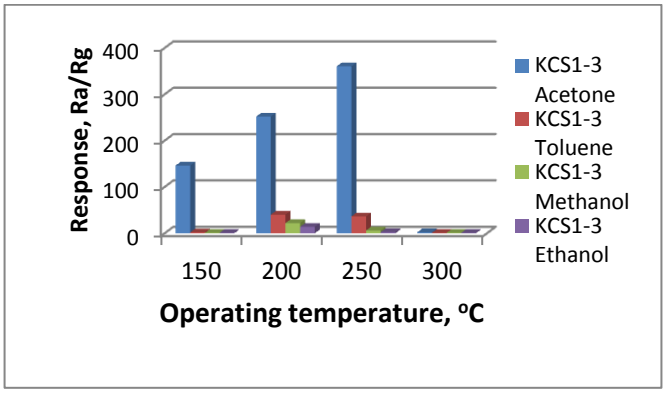

Fig. 6. The responses of specimens on KCS1-3 set of samples to studied VOCs exposure vs operating temperature.

As for EKCS3-2 set of samples made by applying of the hybrid technology, we should be noted that the high response to acetone and toluene vapors of these sensors appears at 200°C but selectivity at that is poor. The selective response to toluene vapors is observed at 150°C (Fig.7). Thus, KCS1-3 and EKCS3-2 series samples functioned at relatively low operating temperature (150°C) could be use as toluene and acetone vapors sensors, respectively.

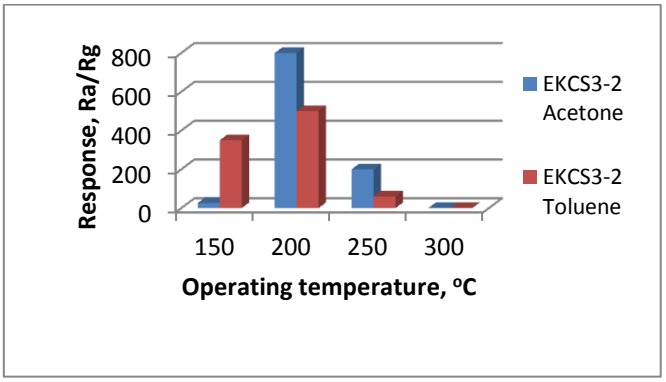

Fig. 7. Response of EKCS3-2 set of samples to 500 ppm acetone and toluene vapors vs operating temperature.

Sufficiently selective response to acetone vapors is registered by ZCS1-200 set of samples at all operating temperatures in the range of 150-300°C. Results of the test measurements are shown in Fig. 8.

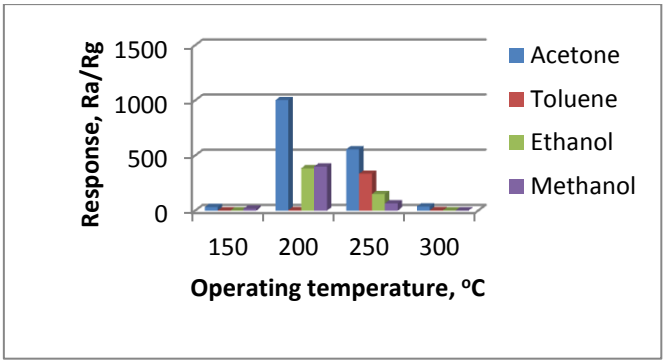

Fig. 8. The responses of specimens on ZCS1-200 set of samples to studied VOCs exposure vs operating temperature.

Data of acetone and toluene responses of considered samples at different operating temperatures are summarized in Table 2.

Response and recovery times are defined from transient response-recovery curves and corresponding dynamic resistance change. As examples, here we adduce some of them for different mentioned above gas sensors. These times to differ for studied sensors. As can see from Fig. 9, the reaction of EKCS3-2 sensors to acetone vapors is rather slow. The recovery at 200°C takes place incompletely. Using pulse supply mode for heater full recovery is reached. But, response and recovery times of KCS1-3 type sensors at 250°C operating temperature and 1000 ppm toluene exposure are about only 24 s and 14 s, respectively (Fig. 10).

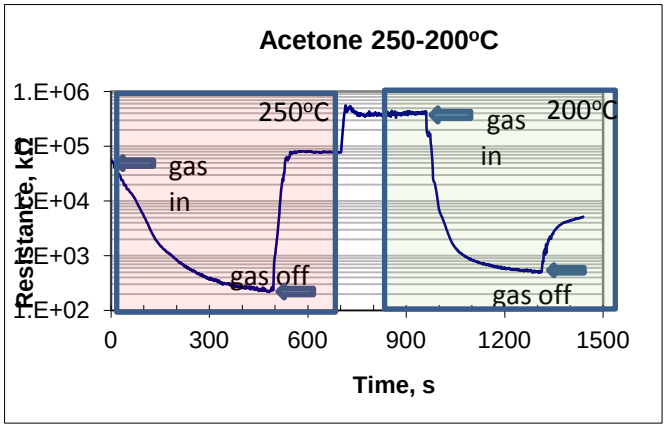

Fig. 9. The response and recovery of EKCS3-2 set of samples to 500 ppm acetone vapors exposure starting at 250°C and then cooling down to 200°C operating temperature.

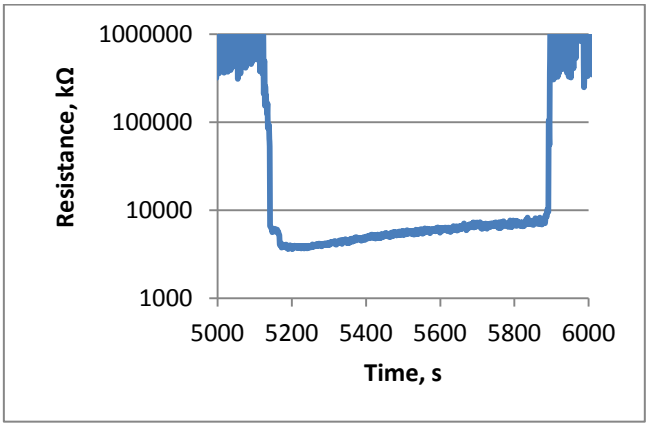

Fig. 10. The response and recovery of KCS1-3 set of samples to 1000 ppm toluene vapors exposure at 250°C operating temperature.

Table 2. Acetone and toluene vapors responses of all studied samples vs operating temperature.

°C	Gas response, R_a/R_g							
	ECS7-2		KCS1-3		EKCS3-2		ZCS1-200	
	Acetone	Toluene	Acetone	Toluene	Acetone	Toluene	Acetone	Toluene
150	2.67	4.88	146.3	2	26.59	350	32.3	1
200	7.62	6.25	251.9	40.21	800	500	1002.34	5
250	86.93	52.96	360.4	84.198	200	60	555.6	334.6
300	46.5	1	2.21	1	1	1	37.5	4.34

The largest response to acetone vapors (R_a/R_g=555,62) in steady-state regime (formed after the first acetone vapor influence) is fixed for ZCS1-200 set of samples with 1:200 mass ratio of the components to 1000 ppm acetone vapors exposure at 250°C operating temperature (Fig. 11). Response and recovery times of these sensors are about 22 and 27 s, respectively.

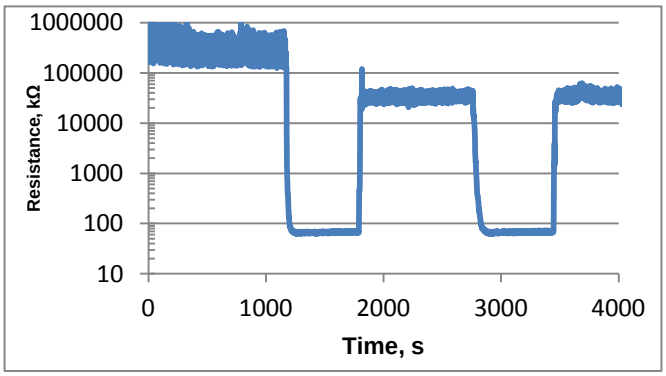

Fig. 11. The response and recovery of ZCS1-200 set of samples to 1000 ppm acetone vapors exposure at 250°C operating temperature.

As an example, the dependence of the ZCS1-200 sensor response vs acetone vapor concentration at 150°C is presented in Fig. 12. Obviously that gas response linearly increases with acetone vapor concentration build up.

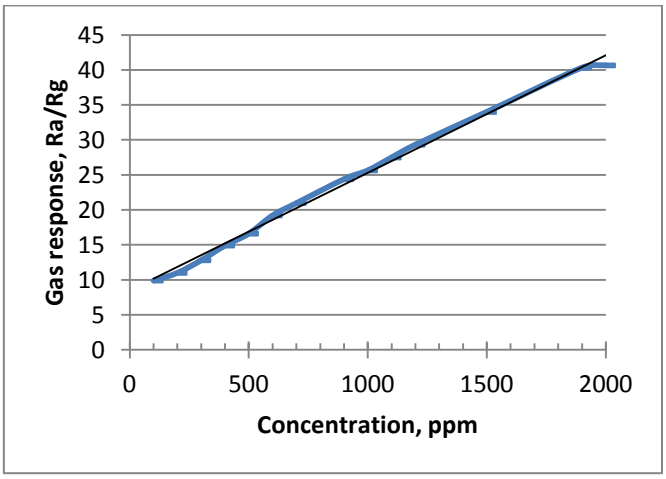

Fig. 12. Dependence of EKCS3-2 sensor response vs acetone vapor concentration.

4. Conclusion

Thus, in this work are found definite conditions at which of studied MWCNTs/SnO_2 nanocomposite gas sensor exhibit the selective reaction to either VOC. So, it is revealed that the nanocomposite structures with 1:4 mass ratio of the components selectively respond to acetone vapors at and acetone and toluene vapors at 150^oC and 250^oC operating temperatures, respectively. Nanocomposite samples with greater mass ratio of the components (1:8, 1:24, 1:50) behave as a very sensitive and selective ethanol and methanol sensors. We can assert that in this range of mass ratio of the nanocomposite components and even for 1:66 and 1:200 one, the sensors made by using the mentioned above hydrothermal synthesis, sol–gel technique and their combined process technologies react to these alcohols something like, e.g. alcohols responses practically not depend from used processing methods. Acetone vapors selective sensitivity of samples with 1:50 mass ratio of the components appears only at the 300^oC operating temperature. The largest and sufficiently selective response to acetone vapors (R_a/R_g more than 1000 at 1000 ppm acetone vapor concentration) is achieved at samples with 1:200 mass ratio of the components.

Acknowledgements

This work supported by NATO EAP.SFPP 984.587 and State Committee of Science MES RA 13-1C075 projects.

References

1. S. Gokhale, T. Kohajda, U. Schlink, “Source apportionment of human personal exposure to volatile organic compounds in homes, offices and outdoors by chemical mass balance and genetic algorithm receptor models,” Sci. Total Environ. 407, pp. 122–138, 2008.
2. S. Wang, H.M. Ang, M.O. Tade, “Volatile organic compounds in indoor environment and photocatalytic oxidation: state of the art,” Environ. Int. 33, pp.694–705, 2007.
3. K. Inyawilert, A. Wisitsoraat, A. Tuantranont, P. Singjai, S. Phanichphant, C. Liewhiran, “Ultra-rapid VOCs sensors based on sparked-In_2O_3 sensing films,” Sensors and Actuators B 192, () 745– 754, 2014.\
4. S.A. Feyzabad, A.A. Khodadadi, M.V. Naseh, Y. Mortazavi, “Highly sensitive and selective sensors to volatile organic compounds using MWCNTs/SnO_2,” Sens. Actuators B 166–167, pp. 150–155, 2012.
5. X. Li, Y. Chang, Y. Long, “Influence of Sn doping on ZnO sensing properties for ethanol and acetone,” Mater. Sci. Eng. C 32, pp. 817–821, 2012.
6. C. Garzella, E. Comini, E. Bontempi, L.E. Depero, C. Frigeri, G. Sberveglieri, “Sol-gel TiO_2 and W/TiO_2 nanostructured thin films for control of drunken driving,” Sens. Actuators B 83, pp. 230–237, 2002.
7. T. Brousse, D.M. Schleich, “Sprayed and thermally evaporated SnO_2 thin films for ethanol sensors,” Sens. Actuators B 31, pp. 77–79, 1996.
8. M. Salaspuro, “Acetaldehyde as a common denominator and cumulative carcinogen in digestive tract cancers,” Scandinavian J. of Gastroenterology, 44 (8), pp. 912–925, 2009.
9. Xue Bai, Huiming Ji, Peng Gao, Ying Zhang, Xiaohong Sun, “Morphology, phase structure and acetone sensitive properties of copper-doped tungsten oxide sensors,” Sens. Actuators B 193, pp. 100–106, 2014.
10. N. Makisimovich, V. Vorotyntsev, N. Nikitina, O. Kaskevich, P. Karabun, F. Martynenko, “Adsorption semiconductor sensor for diabetic ketoacidosis diagnosis,” ,Sens. Actuators B 35–36, pp. 419–421, 1996.
11. L. Wang, A. Teleki, S.E. Pratsinis, P.I. Gouma, Ferroelectric WO_3 nanoparticles for acetone selective detection, Chem. Mater. 20, pp. 4794–4796, 2008.

12. J. Lerchner, D. Caspary, G. Wolf, "Calorimetric detection of volatile organic compounds," Sens. Actuators B: Chem. 70, pp. 57–66, 2000.
13. M. Consales, A. Crescitelli, M. Penza, P. Aversa, P.D. Veneri, M. Giordano, A. Cusano, "SWCNT nanocomposite optical sensors for VOC and gas trace detection," Sens. Actuators B: Chem. 138, pp. 351–361, 2009.
14. T. Sasahara, H. Kato, A. Saito, M. Nishimura, M. Egashira, "Development of a ppb level sensor based on catalytic combustion for total volatile organic compounds in indoor air," Sens. Actuators B: Chem. 126, pp. 536–543, 2007.
15. M. Hanada, H. Koda, K. Onaga, K. Tanaka, T. Okabayashi, T. Itoh, H. Miyazaki, "Portable oral malodor analyzer using highly sensitive In_2O_3 gas sensor combined with a simple gas chromatography system," Anal. Chim. Acta 475, pp. 27–35, 2003.
16. C. Xu, J. Tamaki, N. Miura, N. Yamazoe, "Grain size effects on gas sensitivity of porous SnO_2-based elements," Sensors and Actuators B 3, pp. 147–155, 1991.
17. G. Korotcenkov, S.-D. Han, B.K. Cho, V. Brinzari, "Grain size effects in sensor response of nanostructured SnO_2- and In_2O_3-based conductometric thin film gas sensor," Critical Reviews in Solid State and Materials Sciences 34, pp. 1–17, 2009.
18. A.Z. Adamyan, Z.N. Adamyan, V.M. Aroutiounian, A.H. Arakelyan, J. Turner, K. Touryan, "Sol–gel derived thin-film semiconductor hydrogen gas sensor," International Journal of Hydrogen Energy 32 pp. 4101–4108, 2007.
19. M. Tonezzer, N.V. Hieu, "Size-dependent response of single-nanowire gas sensors," Sensors and Actuators B 163, pp. 146–152, 2012.
20. Wang, L.F. Zhu, Y.H. Yang, N.S. Xu, G.W. Yang, "Fabrication of a SnO_2 nanowire gas sensor and sensor performance for hydrogen," Journal of Physical Chemistry C 112, pp. 6643–6647, 2008.
21. L.P. Qin, J.Q. Xu, X.W. Dong, Q.Y. Pan, Z.X. Chen, Q. Xiang, F. Li, "The template free synthesis of square-shaped SnO_2 nanowires: the temperature effect and acetone gas sensors," Nanotechnology 19, pp. 185705, 2008.
22. X.M. Han, B. Zhang, S.K. Guan, J.D. Liu, X. Zhang, R.F. Chen, "Gas-sensing properties of SnO_2 nanobelts synthesized by thermal evaporation of Sn foil," Journal of Alloys and Compounds 461, pp. L26–L28, 2008.
23. Youngjae Kwon, Hyunsu Kim, Sangmin Lee, In-Joo Chin, Tae-Yeon Seong, Wan In Lee, Chongmu Lee, "Enhanced ethanol sensing properties of TiO_2 nanotube sensors," Sensors and Actuators B 173, pp. 441– 446, 2012.
24. Yi-Jing Li, Kun-Mu Li, Chiu-Yen Wang, Chung-I. Kuo, Lih-Juann Chen, "Low-temperature electrodeposited Co-doped ZnO nanorods with enhanced ethanol and CO sensing properties," Sensors and Actuators B 161, pp. 734–739, 2012.
25. Y. Tan, C.C. Li, Y. Wang, J.F. Tang, X.C. Ouyang, "Fast-response and high sensitivity gas sensors based on SnO_2 hollow spheres," Thin Solid Films 516, pp. 7840–7843, 2008.
26. Cheng, S.Y. Ma, X.B. Li, J. Luo, W.Q. Li, F.M. Li, Y.Z. Mao, T.T. Wang, Y.F. Li, "Highly sensitive acetone sensors based on Y-doped SnO_2 prismatic hollow nanofibers synthesized by electrospinning," Sensors and Actuators B 200, pp. 181–190, 2014.
27. Lin Mei, Jiwei Deng, Xiaoming Yin, Ming Zhang, Qiuhong Li, Endi Zhang, Zhi Xu, Libao Chen, Taihong Wang, "Ultrasensitive ethanol sensor based on 3D aloe-like SnO_2," Sensors and Actuators B 166–167, pp. 7–11, 2012.
28. L. Zhao, M. Choi, H.-S. Kim, S.-H. Hong, "The effect of multiwalled carbon nanotube

doping on the CO gas sensitivity of SnO_2-based nanomaterials," Nanotechnology, 18, pp. 445501, 2007.

29. Sadegh Ahmadnia-Feyzabad, Abbas Ali Khodadadia, Masoud Vesali-Naseh, Yadollah Mortazavi, "Highly sensitive and selective sensors to volatile organic compounds using MWCNTs/SnO_2," Sensors and Actuators B 166–167, pp. 150–155, 2012.
30. V.M. Aroutiounian, A.Z. Adamyan, E.A. Khachaturyan, Z.N. Adamyan, K. Hernadi, Z. Pallai, Z. Nemeth, L. Forro, A. Magrez, "Methanol and ethanol vapor sensitivity of MWCNT/SnO_2/Ru nanocomposite structures," In Proc. of the 14th Int. Meeting on Chemical sensors, pp. 1085-1088, 2012.
31. **V**.M. Aroutiounian, A.Z. Adamyan, E.A. Khachaturyan, Z.N. Adamyan, K. Hernadi, Z. Pallai, Z. Nemeth, L. Forro, A. Magrez, E. Horvath, "Study of the surface-ruthenated SnO_2/MWCNTs nanocomposite thick-film gas sensors," Sensors and Actuators B 177, pp. 308–315, 2013.
32. P. Berki, Z. Németh, B. Réti, O. Berkesi, A. Magrez, V. Aroutiounian, L. Forró, K. Hernadi, "Preparation and characterization of multiwalled carbon nanotube/In_2O_3 composites," Carbon 60, pp. 266-272, 2013.
33. N.V. Hieu, L.T.B. Thuy, N.D. Chien, "Highly sensitive thin film NH_3 gas sensor operating at room temperature based on SnO_2/MWCNTs composite," Sensors and Actuators B 129, pp. 888–895, 2008.
34. Y.-L. Liu, H.-F. Yang, Y. Yang, Z.-M. Liu, G.-L. Shen, R.-Q. Yu, "Gas sensing properties of tin dioxide coated carbon nanotubes," Thin Solid Films 497, pp. 355–360, 2006.
35. B.-Y. Wei, M.-C. Hsu, P.-G. Su, H.-M. Lin, R.-J. Wu, H.-J. Lai, "A novel SnO_2 gas sensor doped with carbon nanotubes operating at room temperature," Sensors and Actuators B 101, pp. 81–89, 2004.
36. G. Korotcenkov, S.H. Han, B.K. Cho, "Material design for metal oxide chemiresistive gas sensors," Journal of Sensor Science and Technology 22(1) pp. 1-17, 2013.
37. E. Couteau, K. Hernadi, J.W. Seo, L. Thien-Nga, Cs. Mikó, R. Gáal, L. Forró, "CVD synthesis of high-purity multiwalled carbon nanotubes using $CaCO_3$ catalyst support for large-scale production," Chem. Phys. Lett., 378, pp. 9-17, 2003.
38. Arnaud Magrez, Jin Won Seo, Rita Smajda, Marijana Mionić, László Forró, "Catalytic CVD Synthesis of Carbon Nanotubes: Towards High Yield and Low Temperature Growth," Materials 3 pp. 4871-4891, 2010.
39. Zoltan Nemeth, Balazs Reti, Zoltan Pallai, Peter Berki, Judit Major, Endre Horvath, Arnaud Magrez, Laszlo Forro, Klara Hernadi, "Chemical challenges during the synthesis of MWCNT-based inorganic nanocomposite materials," Phys. Status Solidi B pp. 1-6, 2014.
40. A.Z. Adamyan, Z.N. Adamyan, V.M. Aroutiounian, A.H. Arakelyan, J. Turner, K. Touryan, Sol-Gel Derived Thin-film Semiconductor Hydrogen Gas Sensor, Int. J. of Hydrogen Energy, 32, pp. 4101-4108, 2007.
41. Thanh Thuy Trinh, Ngoc Han Tu, Huy Hoang Le, Kyung Yul Ryu, Khac Binh Le, Krishnakumar Pillai, Junsin Yi, "Improving the ethanol sensing of ZnO nano-particle thin films-The correlation between the grain size and the sensing mechanism," Sensors and Actuators B 152, pp. 73–81, 2011.